HIGH EFFICIENT LED FOR WHITE LIGHT

M. Nazarov, C. Yoon

Samsung Electro-Mechanics Co, LTD, Metan 3-Dong, Yeogtong-Gu, Suwon, Republic of Korea

Abstract

The highly efficient red-emitting phosphors $(Ca_{1-x}Sr_x)S:Eu^{2+}$ and $(Ca_{1-x}Sr_x)Se:Eu^{2+}$, in combination with commercial green phosphor $SrGa_2S_4:Eu^{2+}$ and blue LED are proposed for a three-band white LED. The luminescence mechanism and optimization parameters are discussed.

Introduction

The development of wide band gap III-V nitride compound semiconductors has led to the commercial production of high-efficiency LEDs [1,2]. The recent advent of blue InGaN technology has made it possible to produce a conventional white LED in which white light is obtained by coating a $Y_3Al_5O_{12}$:Ce (YAG) or $Tb_3Al_5O_{12}$:Ce (TAG) phosphor onto a blue LED chip [3-6]. In this device, known as a two-band white LED, white light is generated by additive color mixing of the blue light emitted by the blue LED and the yellow light emitted by the YAG or TAG phosphors. The development of a white LED is important because it opens the way for LED applications such as light bulbs and fluorescent lamps with high durability and low energy consumption. However, the spectral composition of the light produced by the conventional two-band white LED differs from that of natural white light, particularly in the red region. The color properties of conventional two-band white LEDs can potentially be improved by adding another component to create a white LED based on three emission bands (a three-band white LED). Blue LEDs have been combined with phosphors to convert part of the blue light to red and green light, to produce white light. Suitable phosphors must have a high efficiency of excitation at about 420-480 nm, and a wide chromaticity zone. A luminescent material absorbs energy in one region of the electromagnetic spectrum and emits radiation energy in another region of the spectrum. Typically, the energy of the photons emitted is lower than the energy of the photons absorbed. Full-color fluorescent display

devices have been developed by using a combination of ZnS:Ag (blue), ZnS:Cu,Al (green), and ZnCdS:Ag (red) phosphors excited by a near-UV LED [7]. In addition, a white light source has been obtained by integrating ZnS:Ag (blue), ZnS:Cu,Al (green), and Y_2O_2S:Eu (red) phosphors, and a UV-LED (350 nm) [8]. White light has also been achieved by combining a blue LED (460 nm) with $SrGa_2S_4$:Eu (green) and SrS:Eu (red) phosphors [9]. In the present work, we investigated the optical properties of a white LED which was obtained by using a blue LED (465 nm) in conjunction with $SrGa_2S_4$:Eu (green) and $(Ca_{1-x}Sr_x)S:Eu^{2+}$ or $(Ca_{1-x}Sr_x)Se:Eu^{2+}$, (red) phosphors. The new red phosphor compositions were chosen over the phosphor used in previous works in order to improve the red color characteristics of the white LED.

Experimental details

Classical inorganic phosphors usually consist of a host lattice with activator ions doped into it in small concentrations, typically a few mole percent or less. Selection of optimum phosphor material (host, dopant and codopant) plus the composition optimization leads to color purity, high brightness, high efficiency and long-term stability. Right synthesis rout and synthesis conditions give suitable powder characteristics.

One example of a phosphor composition for a three-band white LED comprises the green-emitting phosphor $SrGa_2S_4:Eu^{2+}$ in combination with at least one of the following red-emitting phosphors consisting of a strontium-calcium sulfide $Ca_{1-x}Sr_xS:Eu^{2+}$ or strontium-calcium selenide $Ca_{1-x}Sr_xSe:Eu^{2+}$, wherein x is a number from 0 to 1. All these phosphors can be synthesized by solid state reaction. By combining the present red phosphors with green phosphor and blue LEDs, full color white light can be obtained. Sometimes the red phosphors could be co-doped by one of halides, for example, Cl.

The red emitting phosphor $Eu^{2+}$and Cl^--doped $(Ca_{1-x}Sr_x)Se$ can be prepared by combining the starting materials: $Sr(NO_3)_2$, $Ca(NO_3)_2 \cdot 4H_2O$, SeO_2 and Eu_2O_3. The host materials, CaSe and SrSe, can be prepared from calcium selenate and strontium selenate, respectively. The phosphors $(Ca_{1-x}Sr_x)Se:Eu^{2+}$ can be synthesized by high temperature solid-state reaction. The stoichiometric amounts of the corresponding raw materials (CaSe, SrSe and EuF_3, which could be prepared by hydrothermal synthesis) have to be thoroughly mixed by grinding in an agate mortar and then heated at 1100 ^oC for 2 h in a stream of reductive atmosphere (N_2+H_2). Fig. 1 shows the general concept of the synthesis process.

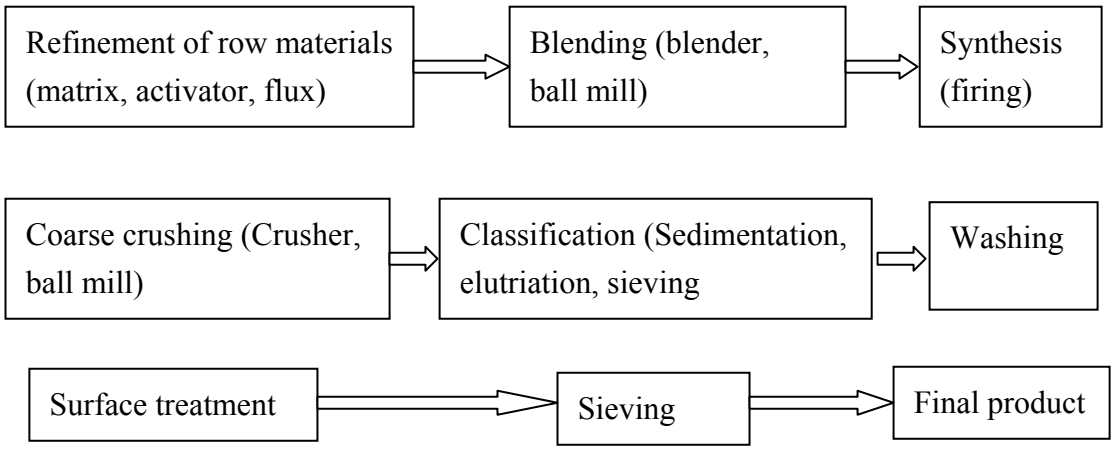

Fig.1. Phosphor synthesis process

Results and discussion

Blue-emitting LEDs are generally known. Usually blue-emitting LED has an emission peak at 420-480, optionally about 450-470 nm. A combination of two blue-excited phosphors (excited by the blue emission from LED), one emitting in the green and one emitting in the red, is used in place of the yellow emitting yttrium aluminum garnet of the Nichia product. Since these new emissions are close to peaks in the tristimulus functions in combination with the blue from the LED they produce light with higher luminous efficacy and better color rendering than the phosphors used in prior devices. These green and red phosphors are selected so that they are excited by the blue-emitting LED. The green color-emitting phosphor typically has an emission peak at 510-550. The red color-emitting phosphor typically has an emission peak at 600-630. The scheme of phosphor converted three-band white LED and emission spectra are presented in fig.2.

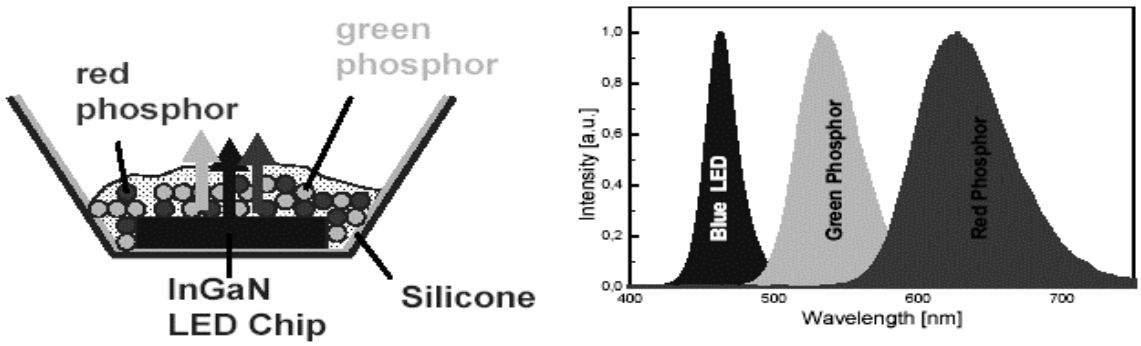

Fig.2. The scheme of phosphor converted three-band white LED.

For commercial green phosphor $SrGa_2S_4:Eu^{2+}$ the excitation spectra consist of broad band in the range of 350-530 nm (Fig.3a). The PL emission spectrum under 450-nm light excitation exhibited a well-known characteristic Eu^{2+} emission with maximum at 530 nm (Fig3b). The FWHM of emission peak is about 50 nm. The emission band is due to the $4f^6 5d^1 \rightarrow 4f^7$ transition of the Eu^{2+} ion.

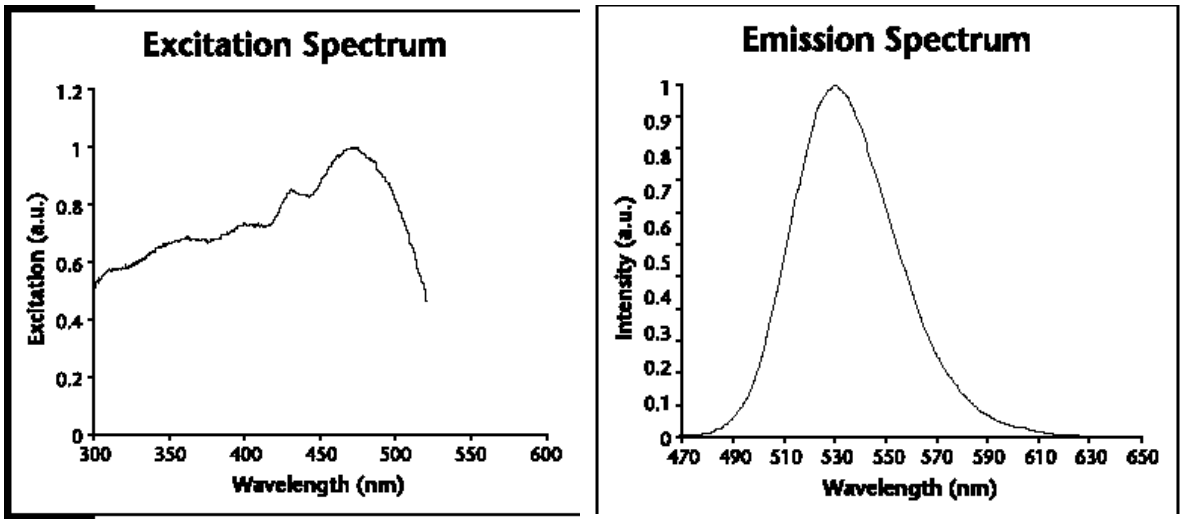

(a) **(b)**

Fig.3 The excitation (a) and emission (b) spectra of $SrGa_2S_4:Eu^{2+}$ (excitation made by 460nm light source).

Reducing the amount of gallium present (for example 6 to 3% excess) reduces the particle size and sometimes the relative efficiency of the $SrGa_2S_4$ phosphor. For example, samples with 6% excess gallium, fired at 1000° C for two hours can have a relative efficiency range from about 65 to 95%, with a median particle size of about 9 microns. A sample with 3% excess gallium, plus the addition of alcohol in the precipitation step fired at 900° C for four hours, can have a relative efficiency of about 80% and a median particle size of about 4 microns.

Figs. 4(a, b) illustrate the excitation and emission spectra of the $(Ca_{1-x},Sr_x)S:Eu^{2+}$ phosphors with different Sr concentrations (x), respectively.

As shown in Fig. 4a, the excitation spectrum (curve 1, λ_{em} = 609 nm) of the phosphor is very broad, this means the phosphor can be well excited by the visible light from 430 to 500 nm, fitting in with blue LED chip. Consequently, the $(Ca_{1-x},Sr_x)S:Eu^{2+}$ phosphor appears red due to the intense absorption of blue light in sunlight. Generally, two types of activator ions can be distinguished and rare-earth phosphors can be separated into two types: broadband emitting owing to the transition between the 5d and 4f (Eu^{2+}, Ce^{3+}) or narrow line emitting owing to the transition of the 4f levels (Eu^{3+}, Tb^{3+}, Tm^{3+}). The first type of activator ions strongly interacts with the host lattice. This is the case when *d* electrons are involved. The strong coupling of the electronic states with vibrational modes of the lattice mainly leads to

more or less broad bands in the spectrum, that we can see in figs.3-5. In the second type the energy levels of the activator ion involved in the emission process show only weak interactions with the host lattice. Typical examples are many of the lanthanide ions Ln^{3+}, where the optical transitions take place solely between *4f* terms that are well shielded from their chemical environment by outer electrons. As a consequence, characteristic line emission spectra can be observed.

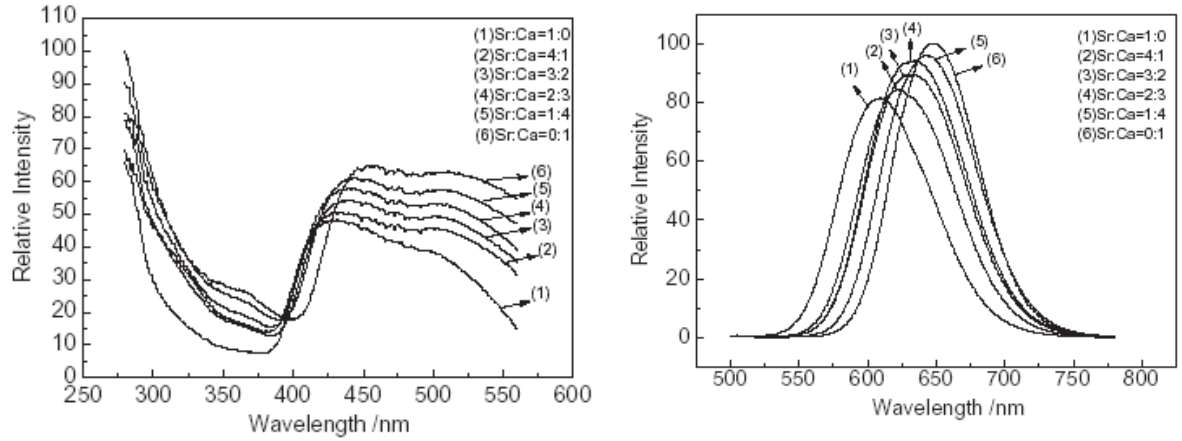

Fig.4. The excitation (a) and emission (b) spectra of $(Ca_{1-x},Sr_x)S:Eu^{2+}$ with different Sr/Ca ratio (excitation made by 460nm light source).

The lowest excited state of 4f levels is located at about $28x10^3$ cm^{-1} [10] and is higher than the $4f^65d^1$ level in most crystals, so that Eu^{2+} usually gives characteristic broadband emission due to transitions between the crystal field components of the $4f^65d^1$ excited state configuration and the $^8S_{7/2}$ ($4f^7$) ground state, which is demonstrated in Fig. 4b (λ_{ex} = 460nm). The wavelength positions of the emission bands depend very much on hosts, changing from the near-UV to the red of the electromagnetic spectrum. This dependence is interpreted as the crystal-field splitting of the 5d level, as shown schematically in Fig. 5.

With the increment of crystal-field strength, the emission bands shift to longer wavelength. As noted above, the $(Ca_{1-x},Sr_x)S:Eu^{2+}$ is a cubic rock-salt structure where Eu^{2+} is on Sr^{2+}/Ca^{2+} sites and is O_h symmetry and small, resulting in the strong crystal field and leading to the red emission. In addition, as illustrated in Figs. 4(a,b), the emission intensity of this phosphor increases by degrees with the Sr concentration (x) from 1 down to 0, and the emission of the phosphor shifts from 609 nm up to 647 nm. Besides the dissimilarity in ionic radius between Sr^{2+} and Ca^{2+}, the energy gaps are 4.41 and 4.30 eV, respectively [11], therefore, the mixing of SrS and CaS makes for the change of the crystal field and energy gap, and accounts for the red shift of the emission wavelength. On this basis, one can vary the Sr/Ca ratio to obtain the desired wavelength.

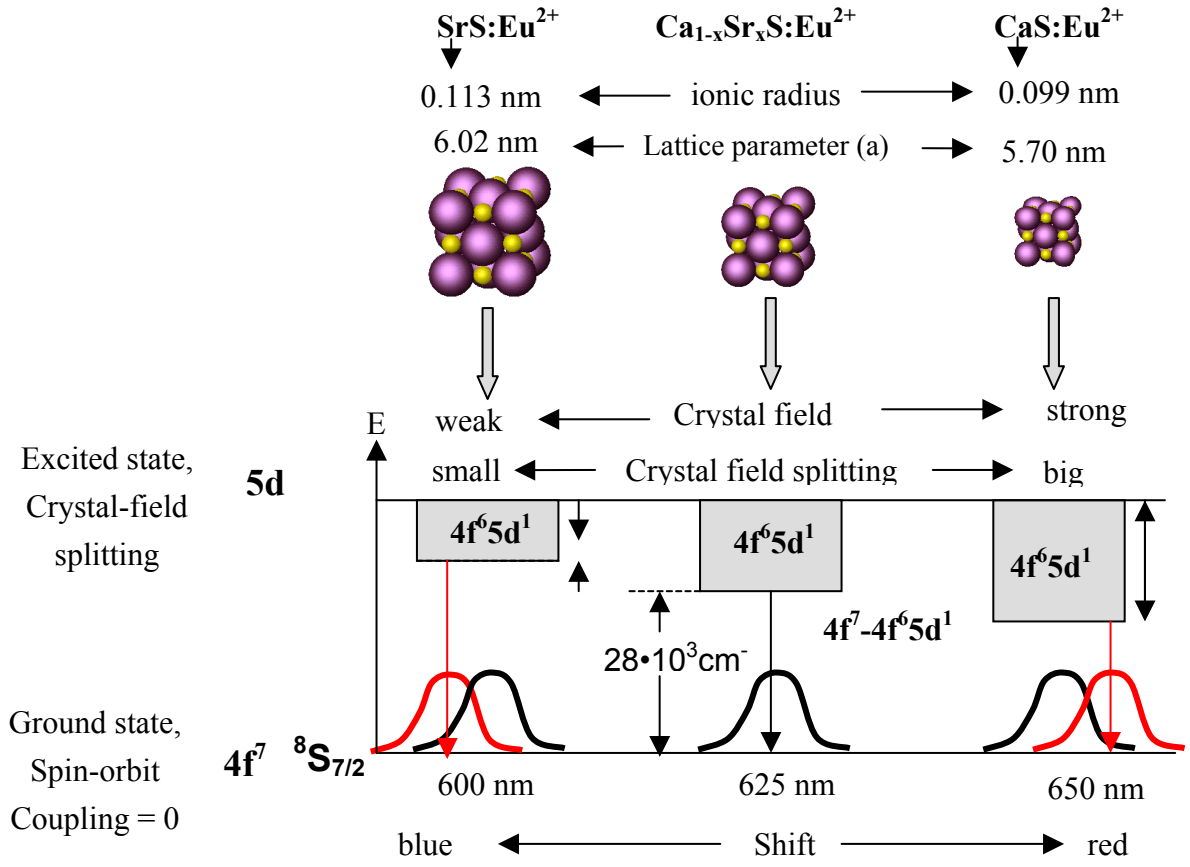

Fig.5. Schematic illustration of crystal field splitting and spectra shift in $(Ca_{1-x},Sr_x)S:Eu^{2+}$ with a different Sr/Ca ratio

The excitation spectra of other proposed red phosphor $(Ca_{1-x}Sr_x)Se:Eu^{2+}$ consist of two broad bands, the low-energy (400–550 nm) and high-energy (250– 350 nm) bands, which are consistent with the diffuse reflectance spectra (Fig.6a). Due to their broadband absorption in the range of 400–550 nm, $(Ca_{1-x}Sr_x)Se:Eu^{2+}$ phosphors can be used to make GaN-based LEDs. The PL emission spectrum under 450-nm light excitation exhibited a well-known characteristic Eu^{2+} emission (Fig.6b). The emission band is due to the $4f^65d^1 \rightarrow 4f^7$ transition of the Eu^{2+} ion. With an increase in (x), the emission band also shifted to shorter wavelength. The peak shift can be explained by the change of crystal field strength as stated above.

Analysis of FWHM (full width at half maximum) of emission peak $(Ca_{1-x}Sr_x)S:Eu^{2+}$ and $(Ca_{1-x}Sr_x)Se:Eu^{2+}$ shows that the FWHM decreases from about 80 nm to about 50 nm when S is substituted by Se (Fig.7). By changing the S/Se ratio we can shift the spectra and vary the FWHM to obtain the desired width. It is good illustrated in Fig.8.

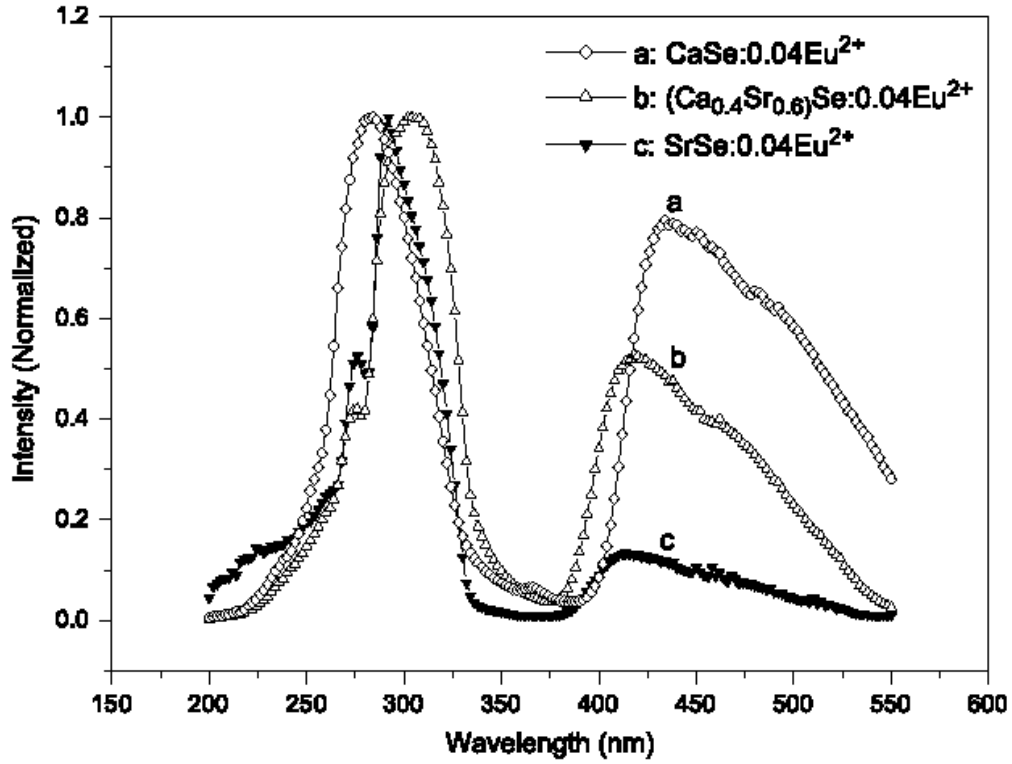

(a)

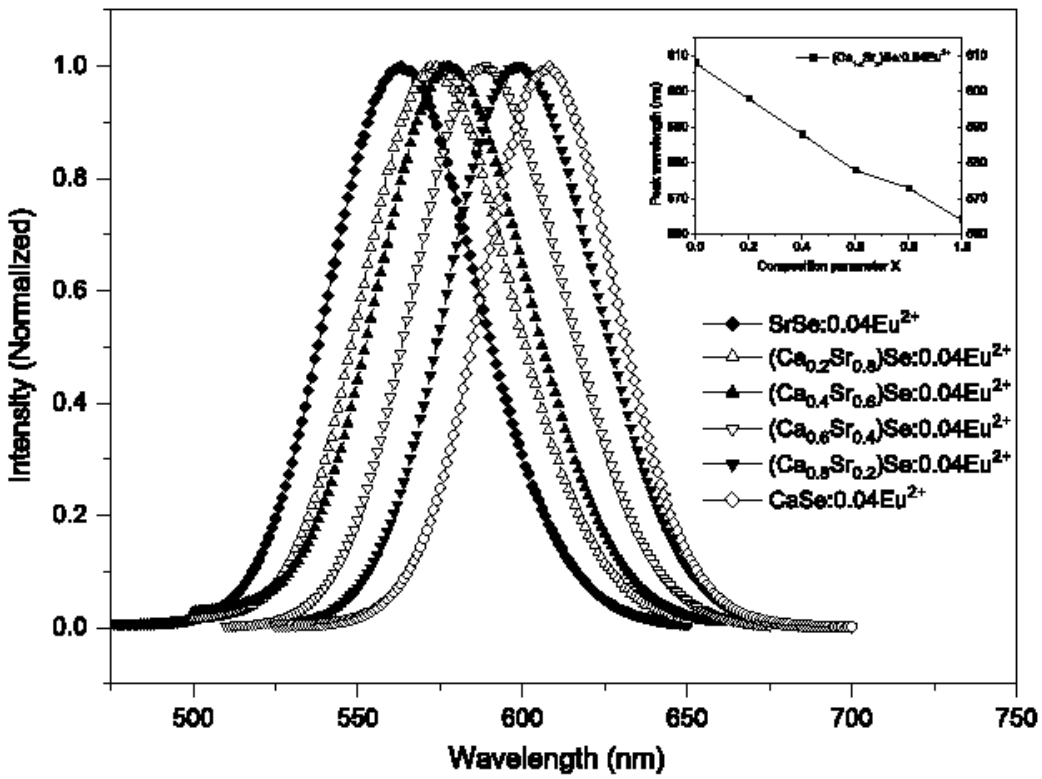

(b)

Fig.6. The excitation (a) and emission (normalized) (b) spectra of $(Ca_{1-x}Sr_x)$ Se: $0.04Eu^{2+}$ with different (x) (λ_{ex}=450 nm). The inset shows the dependence of peak wavelength on the composition parameter (x).

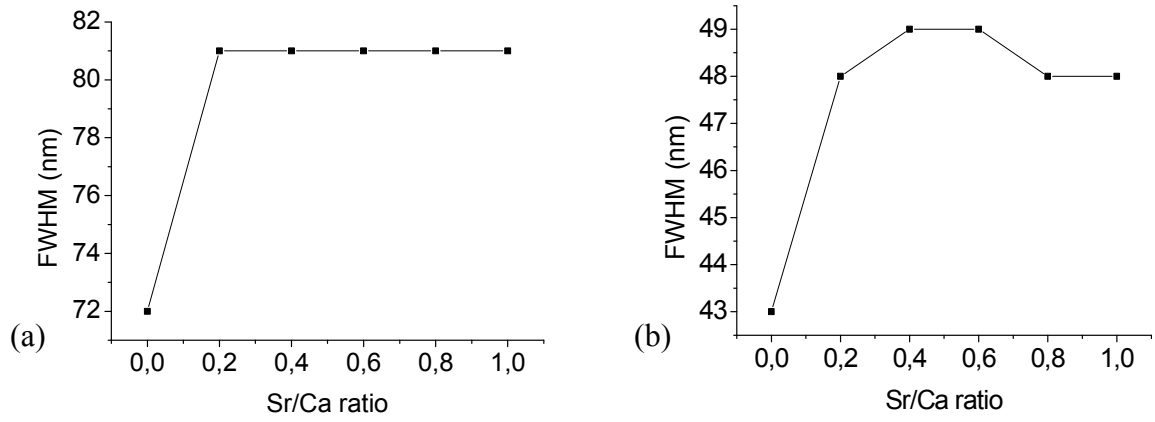

Fig.7. Dependence of FWHM on Sr/Ca ratio in $(Ca_{1-x}Sr_x)S:Eu^{2+}$ (a) and $(Ca_{1-x}Sr_x)Se:Eu^{2+}$ (b)

Selenium has a lower reactivity and vapour pressure with respect to sulphur and is therefore easier to evaporate with limited contamination of the vacuum apparatus. Moreover, Se is completely soluble in the sulphide lattice, leading to the solid solutions $CaS_{1-x}Se_x$ and $SrS_{1-x}Se_x$. Upon increasing coevaporation, the crystal environment of the Eu activator ions gradually changes from CaS to CaSe and from SrS to SrSe. Therefore, taking into account that ionic radius of S is 1.84 Å and Se is 1.98 Å, it can be expected that the photoluminescence emission spectra also change as well as HWHM (Fig.8)

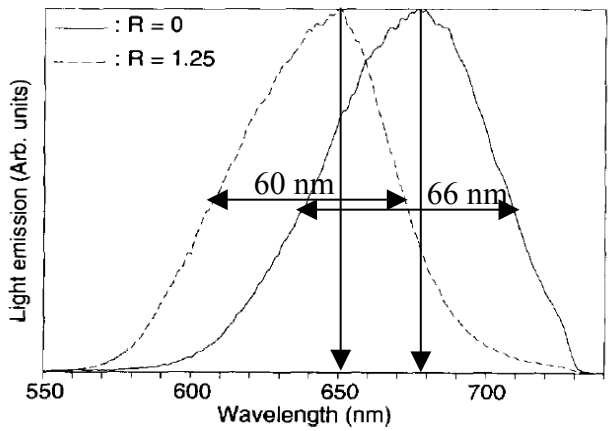

Fig. 8. Emission spectrum of $CaS_{1-x}Se_x$: Eu as a function of S/Se ratio. R=0 corresponds to x=0 and CaS: Eu composition. R=1.25 corresponds to x=0.45 and $CaS_{0.55}Se_{0.45}$: Eu

The inclusion of chlorine in the host lattice increases the intensity and wavelength of emitted red light. The incorporated Cl^- substitutes the host anion S^{2-} or Se^{2-} in corresponding compositions. The Cl^- anion impurities can be incorporated into the host materials when using certain chlorides with low melting temperature as flux in the synthesis of phosphors. The Cl^- impurity in $(Ca_{1-x}Sr_x)S:Eu^{2+}$ or $(Ca_{1-x}Sr_x)Se:Eu^{2+}$ originates in the synthesis process from at least one of the Cl containing fluxes NH_4Cl or $BaCl_2$, for example. The changes in the optical spectra are ascribed to the additional field splitting of the $4f^65d$ state of Eu^{2+} in the distorted

lattice field by incorporation of Cl^-, which replaces one of the six ligand ions of S^{2-} or Se^{2-} and lowers the symmetry of the Eu site from O_h to C_{4v}. The CaS host has a NaCl type of cubic structure. Eu^{2+} ions are commonly believed to substitute the Ca^{2+} cations of the CaS host. Thus, a Eu^{2+} ion in the CaS host is surrounded by six S^{2-} anions, e.g., optical electrons of the activator Eu^{2+} ion are in the octahedral field. The Cl^- anions left in the host lattice generally replace the S^{2-} anions, and the replacement causes changes of the local crystal field. The nearest-neighbor arrangement of Eu^{2+} ion is shown in Fig. 9. In the figure, A represents that there is no Cl^- substitution, O_h symmetry; B represents that there is one Cl^- substitution, C_{4v} symmetry.

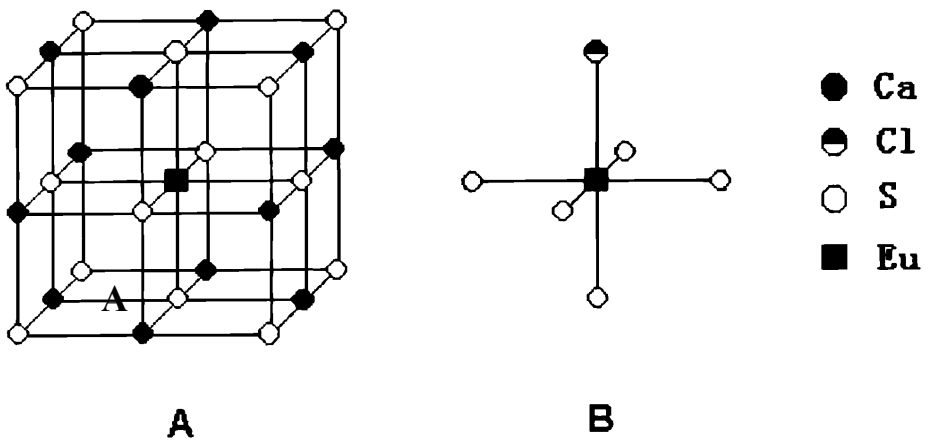

Fig.9. The atomic environment of Eu^{2+} ion. (A) pure CaS:Eu^{2+} without Cl^- substitution, O_h symmetry, (B) with one Cl^- substitution, C_{4v} symmetry.

The luminescent emission spectra of CaS:Eu^{2+} and CaS:Eu^{2+}, Cl^- are shown in Fig. 10. They are measured at room temperature (290 K) by UV excitation. Clearly, the emission shifts from 655 nm for CaS:Eu^{2+} to 670 nm for CaS:Eu^{2+},Cl^-. The emissions of both samples result from the transition from the lowest field splitting component of the $4f^65d^1$ excited state to its $4f^7$ ground state. Using Cl in the flux, it helps the best incorporation of activator in the host lattice and increases the luminescence

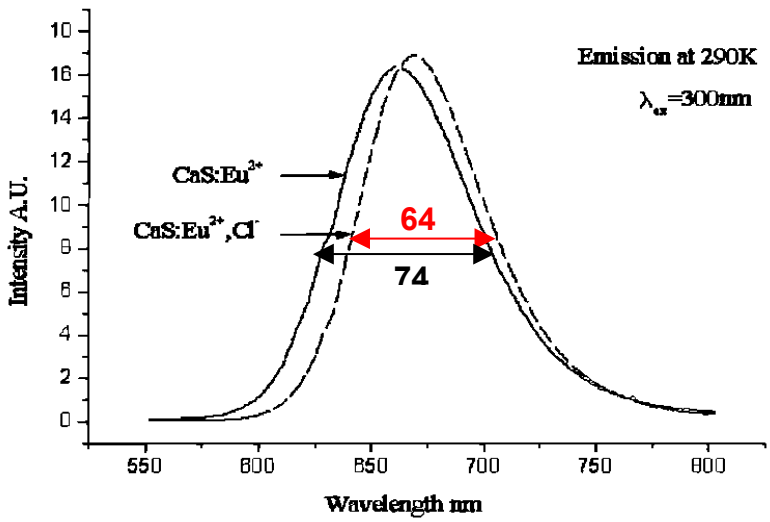

Fig.10. Emission spectra (290 K) of CaS:Eu^{2+} and CaS:Eu^{2+},Cl^-, λ_{ex} = 300 nm. (Dashed curve CaS:Eu^{2+},Cl^- ; solid curve CaS:Eu^{2+}.)

CaSe and SrSe have a cubic unit cell with a=5.912 Å for CaSe and a=6.232 Å for SrSe. The crystal structures of the obtained phosphors $(Ca_{1-x},Sr_x)S:Eu^{2+}$ and $(Ca_{1-x}Sr_x)Se$: $0.04Eu^{2+}$ were examined using the X-ray diffraction. The CaSe–SrSe system was found to be completely miscible in the whole range (x=0 to x=1.0) and the added europium had no influence on the crystal structure of CaSe–SrSe system. Variation in lattice constant is shown as a function of compositional ratio (x) in Fig. 11. It can be seen that Vegard's law holds.

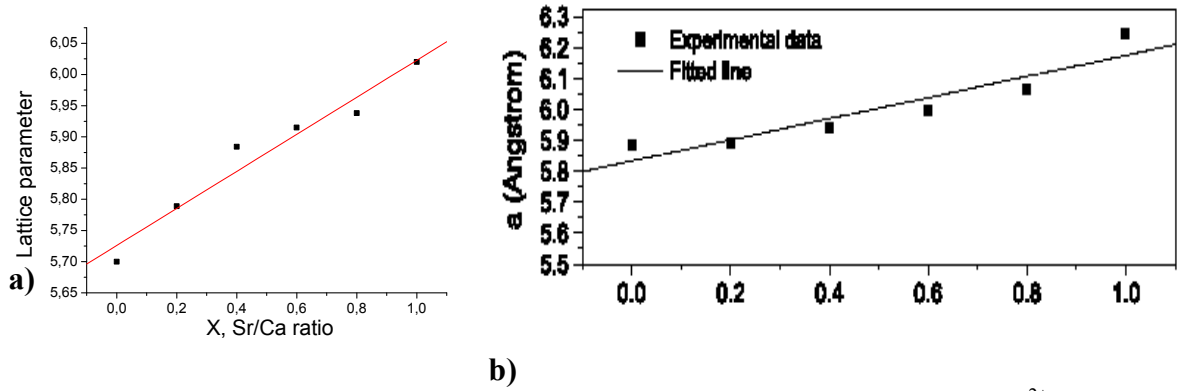

Fig.11. Dependence of lattice constant on compositional ratio (x) in $(Ca_{1-x},Sr_x)S:Eu^{2+}$ (a) and $(Ca_{1-x}Sr_x)Se:0.04Eu^{2+}$ (b) phosphors.

From measuring the lattice parameter the linear peak wavelength dependence on the lattice constant for both phosphors $(Ca_{1-x},Sr_x)S:Eu^{2+}$ and $(Ca_{1-x}Sr_x)Se:Eu^{2+}$ phosphors was established (Fig.12)

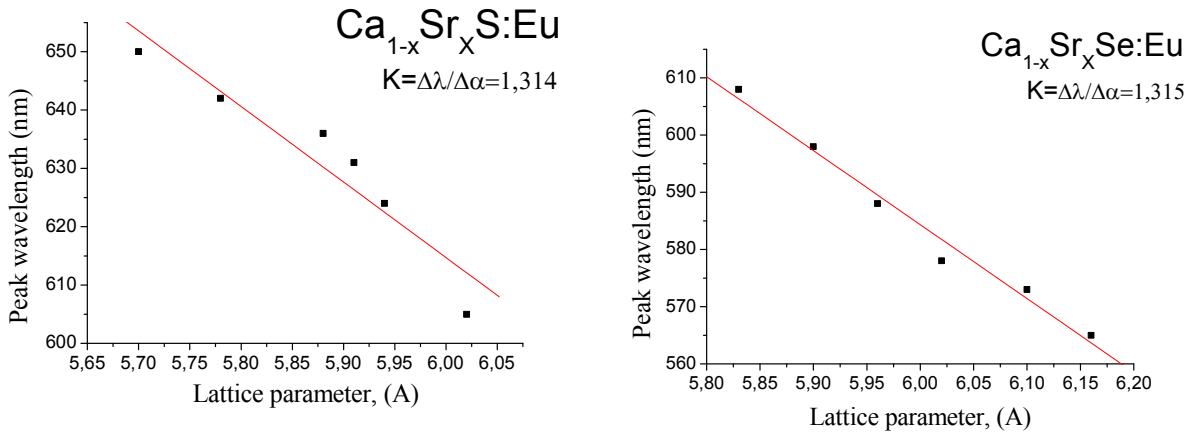

Fig.12 Dependence of peak wavelength on the lattice constant for $(Ca_{1-x},Sr_x)S:Eu^{2+}$ and $(Ca_{1-x}Sr_x)Se:Eu^{2+}$

Upon application of a current, the LED produces a blue light, at least a portion of which is converted to red light and green light. The combination of blue, red, and green light produces a pleasing white light having a preferred combination of parameters such as a color temperature of between 3000^o K and 6500^o K, a CRI of greater than 80, and a device luminous efficacy of 10-20 lumens per watt of input electric power.

Conclusions

The $(Ca_{1-x},Sr_x)S:Eu^{2+}$ and $(Ca_{1-x},Sr_x)Se:Eu^{2+}$ red-emitting phosphors were prepared by solid-state reaction at high temperatures in CO atmosphere. When the sulfide is adopted as starting material, the product is purer than that prepared from sulfate.

(1) These phosphors can be excited efficiently by visible light from 430 to 490nm and emit red light with broadband, which is in agreement with the blue LED chips.

(2) The luminescence originates from the doped Eu^{2+} that replaces the Sr/Ca sites in crystal and acts as the luminescence center.

(3) With the Sr/Ca ratio decreasing, the lattice parameters get lower, and the emission wavelength shows red shift. Suitable wavelength can be got by adjusting the Sr/Ca ratio.

(4) Compared with the commercial afterglow sulfide phosphor, the present synthesized phosphors have higher emission efficiency and are a favorable choice for white LED.

(5) These phosphors exhibit desirable secondary properties in white LED.

Author details

Dr. M. Nazarov, Principal researcher of Samsung Electro-Mechanics Co, LTD, Metan 3-Dong, Yeogtong-Gu, Suwon, Republic of Korea e-mail: mvnazarov@mail.ru

References

[1] S. Nakamura, M. Senob, N. Iwasa, S. Nagahama, T. Yamada, T. Mukai, Jpn. J. Appl. Phys. 1995, 34, L1332.
[2] S. Nakamura, M. Senob, N. Iwasa, S. Nagahama, Appl. Phys. Lett. 1995, 67, 1868.
[3] P. Schlotter, J. Baur, Ch. Hielscher, M. Kunzer, H. Obloh, R. Schmidt, J. Schneider, Mater. Sci. Eng. 1999, B59, 390.
[4] J.H. Yum, S.Y. Seo, S. Lee, Y.E. Sung, J. Electrochem. Soc. 2003, 150, H47.
[5] M. Nazarov. Moldavian Journal of the Physical Sciences, 2005
[6] T. Tamura, T. Setomoto, T. Taguchi, J. Lumin. 2000, 87-89, 1180.
[7] Y. Sato, N. Takahashi, S. Sato, Jpn. J. Appl. Phys. 1996, 35, L838.
[8] T. Nishida, T. Ban, N. Kobayashi, Appl. Phys. Lett. 2003, 82, 3817.
[9] R. Mueller-Mach, G.O. Mueller, M.R. Krames, T. Trottier, IEEE J. Quant. Elect. 2002, 8, 339.
[10] S. Shionoya, W.M. Yen (Eds.), Phosphor Handbook, CRC Press, New York, 1998.
[11] T. Shosaku, J. Lumin. 40–41 (1988) 20.